Available online at www.sciencedirect.com
ScienceDirect
Talanta 71 (2007) 276–281
Talanta
www.elsevier.com/locate/talanta

Aminopolycarboxyl-modified Ag_2S nanoparticles: Synthesis, characterization and resonance light scattering sensing for bovine serum albumin

Hongcheng Pan [a], Xiancong Tao [a], Changjie Mao [a], Jun-Jie Zhu [a,*], Fupei Liang [a,b,*]

[a] *Key Laboratory of Analytical Chemistry for Life Science, School of Chemistry and Chemical Engineering, Nanjing University, Nanjing 210093, China*
[b] *School of Chemistry and Chemical Engineering, Guangxi Normal University, Guilin 541004, China*

Received 29 December 2005; received in revised form 28 March 2006; accepted 30 March 2006
Available online 2 May 2006

Abstract

A novel method was proposed to prepare a series of functionalized Ag_2S nanoparticles capped with various aminopolycarboxylic acids. The as-prepared Ag_2S nanoparticles were characterized by UV–vis, FTIR, resonance light scattering spectra (RLS) and transmission electron microscopy (TEM). Based on the RLS intensities enhanced by BSA-induced Ag_2S nanoparticles aggregation, a sensitive RLS method for the detection BSA at nanogram levels was established. The detection limits for BSA are between 8.6 and 112.6 ng mL^{-1}, depending on the different capping agents. The effects of various capping agents on the detection limits of BSA have been investigated. The detection limit is found to be dependent on the stability constant ($\log K_{MY}$) of the silver–aminopolycarboxyl complexes.

Keywords: Ag_2S nanoparticles; Resonance light scattering; Bovine serum albumin

1. Introduction

The surface-modification of the nanoparticles has attracted special attention because it provides a strategy for selective tailoring the nanoparticles of different surface physical and chemical properties. It allows the functionalized nanoparticles extensive applications in different fields, ranging from biosensing to biolableing. Oligonucleotide-modified nanoparticles and sequence-specific particle assembly events, induced by target DNA, were used to generate materials with unusual optical properties [1,2]. By using various ligands, some functionalized nanoparticles can be attached to special biomolecules such as sugars [3], peptides [4], proteins [5], and DNA [6].

Resonance light scattering technique (RLS), pioneered by Pasternack et al., has been used to investigate porphyrin assemblies on DNA [7]. As a new spectral technique, the resonance light scattering measurements are very simple and sensitive by using a common spectrofluorometer. Yguerabide and Yguerabide demonstrated the light scattering power of a 60-nm gold particle is equivalent to about 5×10^5 fluorescein molecules [8]. In the past decade, RLS spectroscopy, including total internal reflected RLS [9], has been successfully applied to detect DNA [7,10,11], protein [12–15], drugs [16], and inorganic substances [17]. Recently, the research interests have been focused on the enhancement of the light scattering signal based on biomolecule-induced nanoparticle aggregation. The nanoparticle-based RLS probes have advantages over conventional dye-based probes because they are chemically stable and do not suffer from photolysis. Bao et al. reported the application of 80-nm-diameter gold RLS particles coated with anti-biotin antibodies for detection of DNA hybridization on cDNA microarrays [18]. By measuring the ratio of scattered light intensities at 560 and 680 nm, Aslan et al. developed a glucose sensing platform by using modified gold colloids [19]. Polyhydroxylated fullerene (C_{60}) derivative, polystyrene–acrylic acid and polyvinyl alcohol keto-derivative nanoparticles have been employed as RLS probes to detect protein [20–22]. Wang et al. prepared a series of mercaptoacetic acid functionalized metal sulfide nanoparticles such as PbS and HgS. A novel assay of γ-globulin, without separation of human serum albumin, is established on the basis of the measurement of enhanced RLS signals resulting from the interaction of protein and functionalized metal sulfide nanopar-

* Corresponding authors. Tel.: +86 25 8359 4976; fax: +86 25 8359 4976.
E-mail address: jjzhu@nju.edu.cn (J.-J. Zhu).

0039-9140/$ – see front matter © 2006 Elsevier B.V. All rights reserved.
doi:10.1016/j.talanta.2006.03.057

ticles [23,24]. The surface-modification of the nanoparticles is currently under intensive research for development of sensitive RLS probes. However, few studies were focused on the influence of the capping molecules on the sensitivity (e.g. detection limits) of RLS technique.

In the present study we develop a novel RLS technique to detect bovine serum albumin (BSA) at nanogram levels, and investigate the effect of the capping agent on the detection limit. A series of functionalized Ag_2S nanoparticles capped with various aminopolycarboxylic acids were prepared and characterized by UV–vis, FTIR, RLS and TEM. The scattering signals of aminopolycarboxyl-modified Ag_2S nanoparticles have been strongly enhanced by the reactions between BSA and Ag_2S nanoparticles. BSA was detected based on the proportional relationship between the enhanced RLS intensities at 468 nm and the concentration of BSA. The detection limits for BSA are between 8.6 and 112.6 ng mL^{-1}, depending on the different capping agents. It was found that the detection limits (DL) for BSA strongly depended on the stability constant ($\log K_{MY}$) of the silver–aminopolycarboxyl complexes. To the best of our knowledge, this is the first description about the relationship between capping molecules and the detection limit (DL) for BSA. The results could be considered to be useful to design nanoparticle-based RLS probes with sufficient sensitivity.

2. Experimental

2.1. Reagents

Diethylenetriaminepentaacetic acid (DTPA, Beijing Chemical Plant, China), triethylenetetraaminehexaacetic acid (TTHA, Shanghai Chemical Reagent Co. Ltd., China), *trans*-1,2-diaminocyclohexanetetraacetic acid (DCTA, Fluka), Ethylenediamine tetraacetic acid (EDTA, Shanghai Chemical Reagent Co. Ltd., China), Ethylene glycol bis(aminoethylether) tetraacetic acid (EGTA, Huzhou Chemical Plant, China), Hydroxyethylethylenediaminetriacetic acid (HEDTA, Shanghai Chemical Reagent Co. Ltd., China), Nitrilotriacetic acid (NTA, Beijing Chemical Plant, China), $AgNO_3$ (Shanghai Chemical Reagent Co. Ltd., China), and $Na_2S{\cdot}12H_2O$ (Shanghai Chemical Reagent Co. Ltd., China) were all used as received. Bovine serum albumin (BSA, Sigma) was directly dissolved in water to prepare stock solutions of 50 μg mL^{-1} and stored at 4 °C. The working solutions were obtained by diluting the stock solutions with water just before use. NaAc–HAc buffer solution was used to adjust the acidity of the aqueous system. All reagents were of analytical grade and used without further purification. Doubly distilled water was used throughout.

2.2. Synthesis

Various aminopolycarboxyl-modified Ag_2S nanoparticles were prepared as follows. In a typical synthesis, 0.2 mmol of aminopolycarboxylic acid (DTPA, TTHA, DCTA, EDTA, EGTA, HEDTA, or NTA) was dissolved in 30 mL solution and the solution was adjusted to pH 9 with 1 M NaOH. Subsequently, 5 mL of 0.04 M (0.02 mmol) $AgNO_3$ was added under stirring, followed the pH was adjusted by 1 M NaOH solution to 9. Afterward, a 10 mL freshly prepared Na_2S solution (0.02 mmol) was injected into the reaction solution while the mixture continued to stir rapidly. The solution rapidly changed to brown and was left for 10 h at room temperature under stirring. The colloidal solution was purified through centrifugation at 5000 rpm for 5 min to remove the large particles and dialysis for 30 h to remove any residual reagents. Then the solution was diluted to 100 mL with doubly distilled water. The as-prepared Ag_2S solutions can be stored for months at room temperature without aggregation. These different aminopolycarboxyl-modified Ag_2S nanoparticles are referred to Ag_2S–DTPA, Ag_2S–TTHA, Ag_2S–DCTA, Ag_2S–EDTA, Ag_2S–EGTA, Ag_2S–HEDTA and Ag_2S–NTA, according to their capping molecules; the size of the Ag_2S nanoparticles are 19, 17, 20, 23, 16, 24 and 18 nm, respectively.

2.3. Apparatus and measurements

UV–vis absorption spectra were measured on a Shimadzu UV-240 spectrophotometer. The transmission electron microscopy (TEM) sample was prepared by depositing a droplet of solution onto a carbon film supported by copper grids. The TEM images were taken on a JEOL JEM-200CX transmission electron microscope, using an accelerating voltage of 200 kV. Fourier transform infrared (FTIR) spectra were recorded with an FTS 165 Bio-Rad FTIR spectrophotometer in the range 4000–400 cm^{-1} on KBr pellets.

The RLS spectra were obtained by synchronously scanning the excitation and emission monochromators (namely, $\Delta\lambda = 0.0$ nm) of Hitachi 850 Fluorescence spectrophotometer (Kyoto, Japan) in the wavelength region from 300 to 700 nm. The intensity of light scattering was measured at the wavelength where the maximum scattering peak is located. Both the intensity measurement and the spectrum scanning of the resonance light scattering were made by keeping the bandpass of the excitation and the emission of the spectrofluorometer at 5.0 nm.

Appropriate amounts of HAc–NaAc buffer solution were mixed with the aminopolycarboxyl-modified Ag_2S solution. Subsequently, an appropriate volume of bovine serum albumin solution was added. The mixture was diluted with doubly distilled water to 5.0 mL and mixed thoroughly. Then, it is allowed to stand for 5 min, before RLS spectra and the enhancement of light scattering intensity at maximum wavelength were measured. The enhancement of light scattering intensity is represented as $\Delta I = I - I_0$, where I and I_0 are the intensity at maximum wavelength of RLS spectra with and without proteins, respectively.

3. Results and discussion

3.1. Absorption spectra

Fig. 1 shows the absorption spectra of the modified Ag_2S nanoparticles. According to the literature, the band gap of bulk silver sulfide is 1 eV (1240 nm), the apparent large blue shift

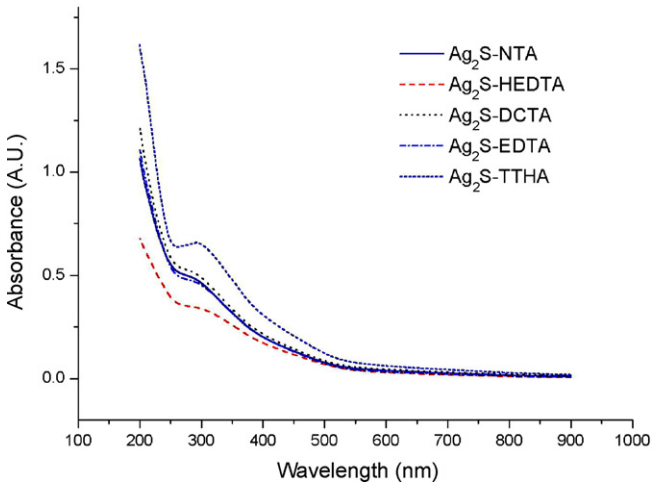

Fig. 1. Absorption spectra of aminopolycarboxyl-modified Ag_2S nanoparticles.

indicates that the nanoparticles are within the quantum confinement regime [25].

3.2. FTIR spectra

To better understand the adsorption mechanism of aminopolycarboxylic acids on the surface of Ag_2S nanoparticles, Fourier transform infrared (FTIR) measurements were carried out. Fig. 2(A) represents the typical IR spectrum of the Ag_2S nanoparticles. Fig. 2(B) reveals that the IR spectrum obtained from the Ag_2S nanoparticles coated with EDTA and others aminopolycarboxyl-modified Ag_2S nanoparticles have the similar IR spectra. It is noted that the C=O stretch band of the carboxyl group located at about 1700 cm^{-1}, is absent in the spectrum of the Ag_2S nanoparticles coated with EDTA. Instead, two new bands at 1560 and 1412 cm^{-1} are characteristic of the asymmetric $\upsilon_{as}(COO^-)$ and the symmetric $\upsilon_s(COO^-)$ stretch. According to the previous investigations, when carboxylic acids adsorb from solution to the metal surface, there may exist two different bonding types of carboxylate groups to the metal, i.e.

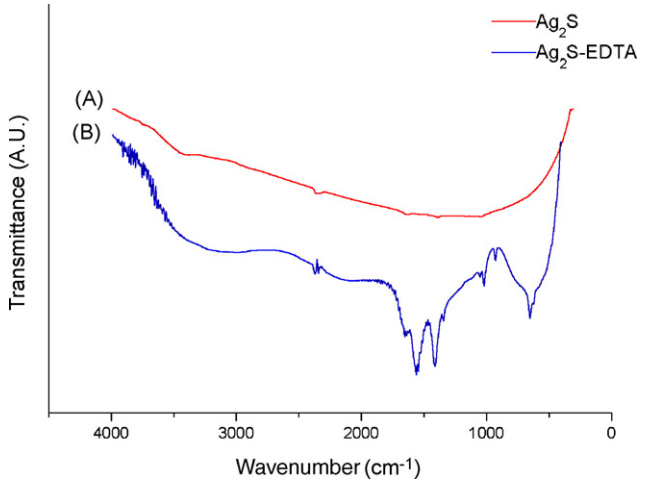

Fig. 2. Representative FTIR spectra of Ag_2S nanoparticles modified with and without EDTA. (A) Ag_2S nanoparticles; (B) Ag_2S nanoparticles modified with EDTA.

either a bidentate bond or a monodentate bond [26,27]. In case of the monodentate bond, the C=O bond, which displays a strong band at about 1700 cm^{-1}, is still present and the metal atoms substitute the acid hydrogen. In the present study, the absence of IR band at 1700 cm^{-1} and two new bands at 1560 and 1412 cm^{-1} demonstrate that EDTA is chemisorbed as a carboxylate onto the surface of Ag_2S nanoparticles. And the two oxygen atoms in the carboxylate are coordinated symmetrically to the Ag atoms.

3.3. TEM images

The typical TEM images for the aminopolycarboxyl-modified Ag_2S nanoparticles are shown in Figs. 3(A) and (C) and 4(A) and (C). It is observed that the particles are well dispersed with a narrow size distribution. TEM images of the aminopolycarboxyl-modified Ag_2S nanoparticles after the addition of appropriate amounts of BSA are shown in Figs. 3(B) and (D) and 4(B) and (D). It is observed that Ag_2S nanoparticles can change from dispersion to aggregation. This indicates the interaction between BSA and the Ag_2S nanoparticles.

3.4. RLS spectral characteristics

Under optimal conditions, both the RLS spectra of aminopolycarboxyl-modified Ag_2S nanoparticles in the absence and presence of BSA have similar features and presented two peaks at 410 and 468 nm. The scattering signals of Ag_2S nanoparticles have been strongly enhanced after adding BSA and these RLS signals increased with the increase the concentration of BSA. As reported in the literature, BSA has a rather weak RLS signal even if its concentration is higher than 20 $\mu g\,mL^{-1}$ [28]. Therefore, the enhancement of the RLS signal suggested that there are the interactions between BSA and the functionalized Ag_2S nanoparticles. The enhancement of the signal can be attributed to the aggregation induced by reaction between carboxyl groups of functionalized Ag_2S nanoparticles and BSA [Ref.]. When surface capped with carbonyl and carboxyl, nanoparticles can bond with the remaining NH_2-groups in proteins. The hydrophobic carbon–carbon skeletal chain of capping molecules can also bond with the hydrophobic amino acid residues. The presence of large aggregation for Ag_2S particles can clearly be observed in the TEM images (Figs. 3 and 4) and thus the inferences can be confirmed. At room temperature, the reactions between functionalized Ag_2S nanoparticles and BSA occur immediately and the time of equilibrium takes only about 5 min. The scattering intensity is stable for atleast 40 min. The maximum wavelength at 468 nm was selected as the optimum for the detection of BSA with high sensitivity. The RLS intensities of functionalized Ag_2S nanoparticles–BSA were found to be proportional to the concentration of BSA, indicating that the detection of BSA with the functionalized Ag_2S nanoparticles is possible.

3.5. Optimization of the general procedures

The optimal conditions such as the effects of pH, concentration of NaAc–HAc buffer solution and Ag_2S nanoparticles

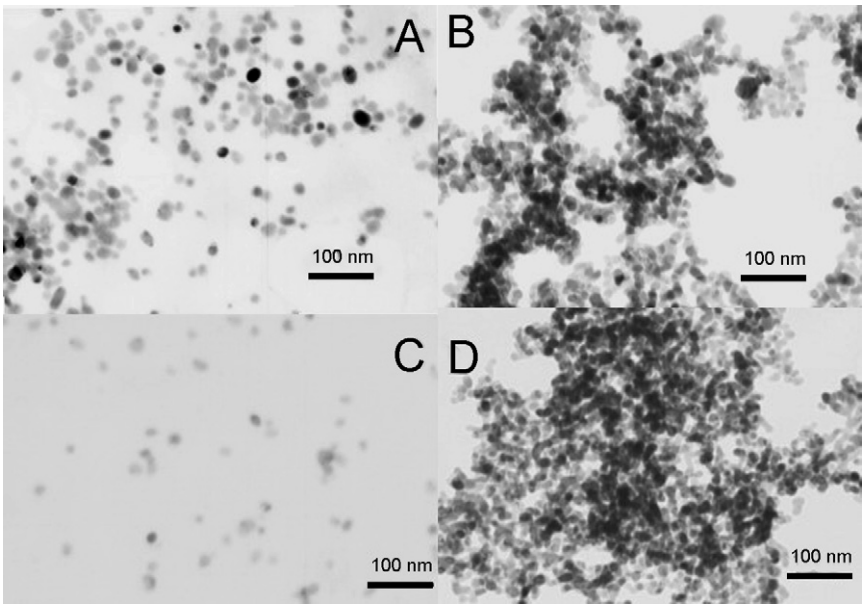

Fig. 3. TEM images: Ag_2S nanoparticles modified with TTHA in the absence (A) and presence (B) of BSA; Ag_2S nanoparticles modified with DCTA in the absence (C) and presence (D) of BSA.

on RLS intensity were investigated. All the optimal conditions are listed in Table 1. Under optimal conditions, BSA was detected based on the proportional relationship between the enhanced RLS intensities at 468 nm and the concentration of BSA. The detection limit is calculated following the equation: $DL = KS_b/S$, where K is a constant related to the confidence level, according to the suggestion of IUPAC, $K = 3$; S_b is the standard deviation of 10 blank measurements, and S is the slope of the calibration curve. As listed in Table 1, the detection limits for BSA are 8.6 ng mL^{-1} for Ag_2S–DTPA, 11.8 ng mL^{-1} for Ag_2S–TTHA, 11.2 ng mL^{-1} for Ag_2S–DCTA, 15.7 ng mL^{-1} for Ag_2S–EDTA, 34.2 ng mL^{-1} for Ag_2S–EGTA, 38.5 ng mL^{-1} for Ag_2S–HEDTA and 112.6 ng mL^{-1} for Ag_2S–NTA, respectively.

3.6. Interferences of coexisting substances and sample determinations

The experiments on the effect of coexisting substances were carried out and the results are shown in Table 2. The results indicated that the method is free from interference from most of amino acids, common metal ions, nucleic acids and glucose. The

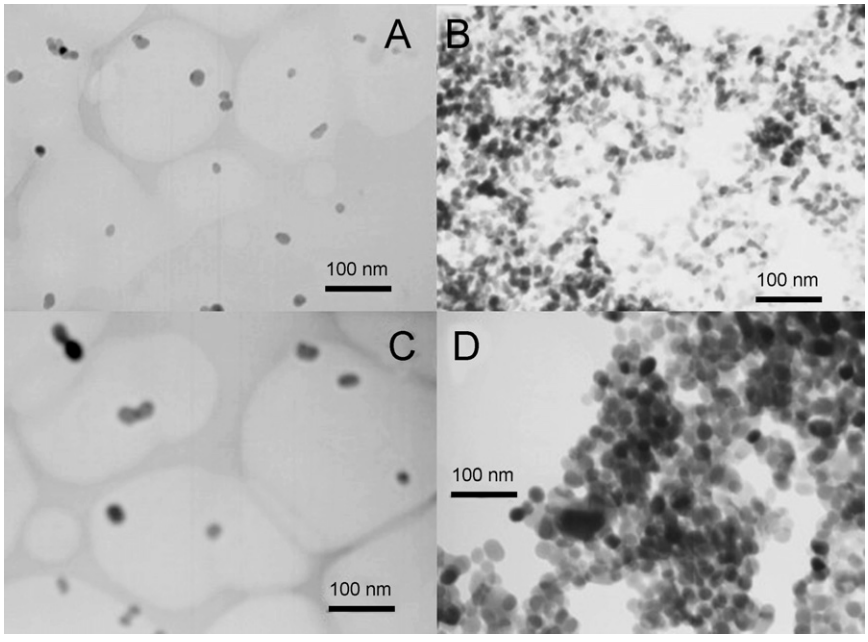

Fig. 4. TEM images: Ag_2S nanoparticles modified with NTA in the absence (A) and presence (B) of BSA; Ag_2S nanoparticles modified with EDTA in the absence (C) and presence (D) of BSA.

Table 1
Optimal conditions of detection BSA using functionalized Ag_2S nanoparticles

	Linear range ($\mu g\,mL^{-1}$)	Detection limit 3σ ($ng\,mL^{-1}$)	Linear regression equation ($ng\,mL^{-1}$)	pH	Concentration of buffer (M)	C_{Ag_2S} (M)	r
Ag_2S–DTPA	0.01–0.12	8.6	$\Delta I = 0.1402C + 7.3302$	4.6	0.05	2×10^{-4}	0.9935
Ag_2S–TTHA	0.02–0.26	11.8	$\Delta I = 0.031C + 2.5586$	4.6	0.04	4×10^{-4}	0.9988
Ag_2S–DCTA	0.03–0.15	11.2	$\Delta I = 0.1791C + 1.3166$	4.6	0.04	2×10^{-4}	0.9935
Ag_2S–EDTA	0.05–0.3	15.7	$\Delta I = 0.1134C + 0.9724$	4.2	0.03	3.2×10^{-4}	0.9834
Ag_2S–EGTA	0.04–0.24	34.2	$\Delta I = 0.0462C + 4.4324$	4.6	0.04	1.2×10^{-4}	0.9847
Ag_2S–HEDTA	0.05–0.5	38.5	$\Delta I = 0.0257C + 4.9394$	4.6	0.04	1.2×10^{-4}	0.9817
Ag_2S–NTA	0.15–0.7	112.6	$\Delta I = 0.0308C + 3.1792$	4	0.03	2×10^{-4}	0.9876

Table 2
Interference of coexisting substances[a]

Coexisting substances	Concentration ($ng\,mL^{-1}$)	Change of $\Delta I_{468\,nm}$ (%)	Coexisting substances	Concentration ($ng\,mL^{-1}$)	Change of $\Delta I_{468\,nm}$ (%)
Glucose	1000	5.6	Na(I), Cl^{-1}	500	1.7
L-tryptophan	500	4.4	K(I), Cl^{-1}	500	3.2
L-cysteine	300	−3.7	Ca(II), Cl^{-1}	300	−5.3
L-phenylalanine	500	5.8	Zn(II), Cl^{-1}	300	−2.8
L-leucine	500	3.2	Mg(II), Cl^{-1}	300	3.3
L-glycine	200	6.7	Pb(II), NO_3^-	100	6.4
fsDNA	500	4.3	Co(II), SO_4^{2-}	100	−3.9

[a] BSA 30 $ng\,mL^{-1}$; Ag_2S–DTPA nanoparticles 2×10^{-4} M; pH 4.6.

Table 3
Analytical results for the diluted cow milk sample[a]

Samples	Content of protein ($mg\,mL^{-1}$)		Recovery $n = 6$ (%)	R.S.D. (%)
	This method	The CBB G-250 method		
Cow milk 1	25.3	23.9	96.5	3.1
Cow milk 2	28.7	29.6	103.1	2.5
Cow milk 3	27.2	28.8	104.6	4.7

[a] Ag_2S–DTPA nanoparticles 2×10^{-4} M; pH 4.6.

real sample determinations were also performed. Table 3 lists the results for the detection of three diluted cow milk samples with the present method. It can be seen that the recovery and relative standard deviation (R.S.D.) are satisfactory and the results are identical to the reference method of CBB G-250 [29].

3.7. Discussion of mechanism

We attribute the enhanced RLS intensities to the aggregation of nanoparticles which was induced by reactions between BSA and aminopolycarboxyl-modified Ag_2S nanoparticles. It was in accordance with the TEM results. In our experiments, BSA (PEI 4.7–4.9) carries a positive charge in the aqueous medium with pH range from 4.0 to 4.6, while the surface of Ag_2S nanoparticles carries negative charges, due to chemisorbed carboxyl groups. The negative charged Ag_2S nanoparticles surface and counterions form an electrostatic double layer that provides a repulsive force enable Ag_2S nanoparticles stable in solution. When aminopolycarboxyl-modified Ag_2S nanoparticles mixed with BSA, positive charged BSA would compress the diffuse double layer around the negative charged Ag_2S nanoparticles, allowing the particles to densely aggregate, thus increasing RLS intensities. No corresponding relationship was found between the size of the as-prepared Ag_2S nanoparticles and the detection limits for BSA. However, we observed the dependence of capping molecules of Ag_2S nanoparticles on the detection limits of BSA. According to the data given by literature, the $\log K_{MY}$ of the silver–aminopolycarboxyl complexes are 5.16 for Ag_2S–NTA, 6.71 for Ag_2S–HEDTA, 7.06 for Ag_2S–EGTA, 7.32 for Ag_2S–EDTA, 8.7 for Ag_2S–TTHA, 8.67 for DTPA, respectively [30]. Compared with the corresponding data for DL, a decline trend of DL with the increase of $\log K_{MY}$ was observed. With a high $\log K_{MY}$ value, the bonding of the aminopolycarboxylic acid and the surface of Ag_2S nanoparticles becomes more stable. As a result the Ag_2S nanoparticles can carry more negative charges. The functionalized Ag_2S nanoparticles with dense negative charges are easily to react with BSA molecules, resulting in the increase of sensitivity in the detection of BSA.

4. Conclusions

In the present study, a novel method to prepare a series of functionalized Ag_2S nanoparticles capped with various aminopolycarboxylic acids was proposed. The as-prepared Ag_2S nanoparticles could be used as RLS probes in response to BSA. Based on the RLS intensities enhanced by BSA-induced Ag_2S nanoparticles aggregation, a sensitive RLS method to detect BSA at nanogram levels was established. The detection limits for BSA are between 8.6 and 112.6 $ng\,mL^{-1}$, depending on the different capping agents. It was found that the dependence of the detection limits for BSA on the stability constant ($\log K_{MY}$) of the silver–aminopolycarboxyl complexes. Although the relationship between capping molecules and detec-

tion limits for BSA is still under study, it is undoubted that the stability of silver–aminopolycarboxyl complexes strongly affects on the detection limits of Ag_2S nanoparticles-based RLS probes.

Acknowledgements

We greatly appreciate the support of the National Natural Science Foundation of China (Grant nos. 20325516, 90206037). This work is also supported by NSFC for Creative Research Group (20521503).

References

[1] C.A. Mirkin, R.L. Letsinger, R.C. Mucic, J.J. Storhoff, Nature 382 (1996) 607.
[2] R. Elghanian, J.J. Storhoff, R.C. Mucic, R.L. Letsinger, C.A. Mirkin, Science 277 (1997) 1078.
[3] T.C. Rojas, J.M. de la Fuente, A.G. Barrientos, S. Penadés, L. Ponsonnet, A. Fernández, Adv. Mater. 14 (2002) 585.
[4] S.R. Whaley, D.S. English, E.L. Hu, P.F. Barbara, A.M. Belcher, Nature 405 (2000) 665.
[5] H. Mattoussi, J.M. Mauro, E.R. Goldman, G.P. Anderson, V.C. Sunder, F.V. Mikulec, M.G. Bawendi, J. Am. Chem. Soc. 122 (2000) 12142.
[6] S.J. Park, A.A. Lazarides, C.A. Mirkin, R.L. Letsinger, Angew. Chem. Int. Ed. 40 (2001) 2909.
[7] R.F. Pasternack, C. Bustamante, P.J. Collings, A. Giannetto, E.J. Gibbs, J. Am. Chem. Soc. 115 (1993) 5393.
[8] J. Yguerabide, E.E. Yguerabide, Anal. Biochem. 262 (1998) 137.
[9] P. Feng, W.Q. Shu, C.Z. Huang, Y.F. Li, Anal. Chem. 73 (2001) 4307.
[10] R. Liu, J. Yang, C. Sun, L. Li, X. Wu, Z. Li, C. Qi, Chem. Phys. Lett. 376 (2003) 108.
[11] X. Long, Q. Miao, S. Bi, D. Li, C. Zhang, H. Zhao, Talanta 64 (2004) 366.
[12] C.Z. Huang, Y. Liu, Y.H. Wang, H.P. Guo, Anal. Biochem. 321 (2003) 236.
[13] R. Jia, H. Zhai, Y. Shen, X. Chen, Z. Hu, Talanta 64 (2004) 355.
[14] H. Zhong, N. Li, F. Zhao, K.A. Li, Talanta 62 (2004) 37.
[15] Y.J. Chen, J.H. Yang, X. Wu, T. Wu, Y.X. Luan, Talanta 58 (2002) 869.
[16] N.B. Li, H.Q. Luo, S.P. Liu, Talanta 66 (2005) 495.
[17] A.H. Liang, Z.L. Jiang, B.M. Zhang, Q.Y. Liu, J. Lan, X. Lu, Anal. Chim. Acta 530 (2005) 131.
[18] P. Bao, A.G. Frutos, C. Greef, J. Lahiri, U. Muller, T.C. Peterson, L. Warden, X. Xie, Anal. Chem. 74 (2002) 1792.
[19] K. Aslan, J.R. Lakowicz, C.D. Geddes, Anal. Chem. 77 (2005) 2007.
[20] G.C. Zhao, P. Zhang, X.W. Wei, Z.S. Yang, Anal. Biochem. 334 (2004) 297.
[21] L.Y. Wang, H.Q. Chen, L. Li, T.T. Xia, L. Dong, L. Wang, Spectrochim. Acta. Part A 60 (2004) 747.
[22] Y. Zhou, S. She, L. Zhang, Q. Lu, Microchim. Acta 149 (2005) 151.
[23] L.Y. Wang, L. Wang, H.Q. Chen, L. Li, L. Dong, T.T. Xia, F.Z. Dong, Z.Q. Xu, Anal. Chim. Acta 493 (2003) 179.
[24] L.Y. Wang, L. Wang, L. Dong, Y.L. Hu, T.T. Xia, H.Q. Chen, L. Li, C.Q. Zhu, Talanta 62 (2004) 237.
[25] M.C. Brelle, J.Z. Zhang, L. Nguyen, R.K. Mehra, J. Phys. Chem. A 103 (1999) 10194.
[26] L.H. Dubois, B.R. Zegarski, R.G. Nuzzo, Langmuir 2 (1986) 412.
[27] N.Q. Wu, L. Fu, M. Su, M. Aslam, K.C. Wong, V.P. Dravid, NanoLetters 4 (2004) 383.
[28] Y.F. Li, C.Z. Huang, X.H. Huang, M. Li, Anal. Sci. 16 (2000) 1249.
[29] D.A. Zhang, Experimental Handbook of Biological Molecules, Jilin University Press, Changchun, China, 1991, p. 327.
[30] L.S. Shen, Handbook of Chemical Analyses and Computation, China Water Power Press, Beijing, China, 1992, p. 227.